INTERNATIONAL JOURNAL OF
COASTAL, OFFSHORE & ENVIRONMENTAL ENGINEERING
IJCOE Vol.8/No. 3/Summer 2023 (1-7)

Available online at: www. Ijcoe.org

The Ultraviolet Index Forecast Using TUV Radiation Model over the Coasts of thePersian Gulf and Oman Sea

Mehdi Rahnama[1], Saviz Sehat Kashani[* 2], Razieh Pahlavan[3], Atefeh Mohammadi[3]

[1]*Assistant Professor, Research Institute of Meteorology and Atmospheric Science, Tehran.*
[2]**Assistant Professor, Research Institute of Meteorology and Atmospheric Science, Tehran; s-sehat@irimo.ir*
[3]*Research Expert, Research Institute of Meteorology and Atmospheric Science, Tehran.*

ARTICLE INFO

Article History:
Received: 03 May. 2023
Accepted: 30 May. 2023

Keywords:
TUV Model
UVI
WACCM
OMI
AOD

ABSTRACT

Ultraviolet radiation can have a significant impact on human health, thus its prediction is necessary and important. In this study, the Tropospheric Ultraviolet and Visible (TUV) Radiation model was used to predict the UltraViolet Index (UVI). This model requires the total ozone column, albedo and Aerosol Optical Depth (AOD) data to forecast UVI. The Global Forecasting System (GFS) data was used for the total ozone column and albedo data, and the Whole Atmosphere Community Climate Model (WACCM) was used for AOD data. In this study, 102 case studies were selected for the coastal stations and islands of the Persian Gulf and Oman Sea in 2019, 2020 and 2021. Due to the lack of access to the actual value of UVI, the Ozone Monitoring Instrument (OMI) data were assumed as observational data. The verification results showed that in the warmer seasons of the year, when UVI levels are higher than in cold seasons, the forecast error is higher. Furthermore, when the AOD value is high, the forecast error is also high, but generally, the forecast is very accurate. For all selected case studies, the ME, MAE, RMSE and R values are -0.81, 1.07, 1.83 and 0.75 respectively, indicating the high accuracy of the UVI forecasts.

1. Introduction

UltraViolet (UV) is a major source of vitamin D in humans. At the same time, excessive exposure to ultraviolet radiation adversely affects humans, animals and plants [1-3]. The effect of ultraviolet light on human skin is discussed by weighting the solar spectrum [4]. The analytical formula presented by McKinley and Diffey [5] was updated and approved as a standard by the l'Eclairage international commission (CIE[1]). The integral (on the wavelength) of solar spectral radiation weighed by the CIE method, is a common criterion for determining the power of solar radiation to cause sunburn. Ultraviolet Index (UVI) is a dimensionless parameter that can reach up to 20 in the high-altitude areas within the tropics [6].

Ultraviolet radiation is defined as electromagnetic radiation with wavelengths in the range of 200-400 nm and is divided into three different bands. UVC is related to the wavelength from 200 to 280 nm, while UVB is related to the wavelength ranging from 280 to 315 nm and UVA is related to the wavelength from 315 nm to the visible level (400 nm). The UVI is an international standard for measuring the radiant power of ultraviolet light on sunburn at specific locations and times. According to the global solar ultraviolet index standard, if this index is on the numbers of 1 and 2, it is safe. Indexes 3, 4 and 5 indicate a low risk and indexes 6 and 7 indicate a high risk. Indexes 8, 9 and 10 indicate a very high risk and an index above 11 indicates a very intensive risk. Therefore, it is necessary to take various protective actions to prevent the damages caused by solar ultraviolet light. Ultraviolet radiation can be predicted by numerical models that include the effects of altitude and distance from the sun, stratospheric ozone, cloud conditions, air pollutants and surface albedo, all of which effect on the amount of ultraviolet radiation reached to the surface.

Ultraviolet light also affects the biosphere [7] including aquatic ecosystems which play an important role in the biochemical cycles [8]. The productivity of phytoplankton is strongly affected by ultraviolet radiation [9], leading to positive or negative feedback on the climate [10].

Simulations of the global circulation model show that the Brewer Dobson Circulation (BDC) will accelerate in the next century [11]. Hence, this leads to a decrease in ozone levels in the tropics and an increase in the

[1] Commission Internationale de l'Eclairage

higher atitudes [12], and so it causes some changes in the amount of UV radiation reaching the earth surface. While the implementation of the Montreal Protocol strongly reduces the emissions of chlorine and bromine gases destructing the ozone layer, recent studies on the evolution of ozone in climate change [11] raise questions about future UV amount [12 13, 14, 15].

Numerous studies of the Chemistry and Climate Model (CCM) have shown an increase in Brewer Dobson circulation (BDC) due to the increase of greenhouse gas concentrations in the atmosphere [12]. BDC was suggested by Brewer [16] and Dobson [17] to explain the geographical distribution of ozone and the amount of water vapor in the stratosphere. BDC refers to the displacement of the meridian in the stratosphere, with air rising in the tropics and subsidence in the polar latitudes. The mechanisms that drive this circulation are Rossby losses and gravitational waves [18]. Therefore, the strength of BDC depends on the propagation and refraction of planetary waves. In addition, rapid loss of Chlorofluorocarbons reduces the ozone regeneration time [19]. BDC amplification and rapid ozone recovery alter the distribution of ozone in the stratosphere and affect ultraviolet light at the surface.

Hegglin and Shepherd [12] predicted a 3.8% increase of UVI in the tropics between 1960 and 2090 in the context of climate change, using stratospheric CCM simulations. Lamy et al. [20] predicted the UVI value for 2010 to 2100 by pairing the Chemistry Climate Model Initiative (CCMI) model with the Tropospheric Ultraviolet and Visible (TUV) model [21], and investigating the effect of climate change on the UVI amount. Moreover, Podrascanin et al. [22] predicted UVI in the Vojvodina region of northern Serbia using an empirical model.

For the first time, a method for UVI prediction in dusty conditions of the Middle East was developed by Roshan et al. [23] who used a three-dimensional mesoscale chemistry-meteorology regional model. They used the WRF-Chem model to predict the Global Horizontal Irradiance (GHI) and estimated the amount of UVI in Doha, Qatar, through the relevant equations. They used the GOCART[2] aerosol scheme and the RACM[3] chemistry scheme in the model. Afterwards, the obtained UVI values were compared with the corresponding values of the Ozone Monitoring Instrument (OMI).

Lamy et al. [24] investigated the changes of ultraviolet radiation using first phase simulations of the CCMI project. CCMI is a project initiated by the International Global Atmospheric Chemistry (IGAC), World Climate Research Programme (WCRP), and Stratosphere-troposphere Processes and their Role in Climate (SPARC). They used the CCMI data and the TUV model to calculate the worldwide surface radiation.

The current UVI operational forecasting models were developed in the 1990s and early 2000s [25]. Krzyścin et al. [25] predicted the ultraviolet radiation from the TUV model using ozone data of the GFS[4] model and ensemble forecast of cloud with the WRF[5] regional model.

In this study, UVI was forecasted for 102 case studies over coastal stations and islands of the Persian Gulf and Oman Sea in the years 2019, 2020, and 2021. The Ozone and albedo data were extracted from the GFS model and Aerosol Optical Depth (AOD) data from the WACCM model as the inputs of the TUV model. In the next step, the outputs of the TUV model were compared with corresponding OMI data. Considering that no research on UVI prediction has been studied in Iran so far, this is the first attempt in this field.

2. Data and methodology

This section introduces the model and data used for UVI forecasting, and also binary verification scores.

2.1. TUV model description

The TUV Radiation model is used to predict the UVI. This model [21] is widely applied by scientific communities for applications such as atmospheric photochemistry, solar radiometry, and environmental photobiology. This model can calculate the spectral radiation, irradiance, and actinic flux at a wavelength of 120-750 nm with a resolution of 0.01 nm. Moreover, spectral weight integrals including wavelength bands (visible, UVA, UVB, UVC), photolysis coefficients (112 reactions), photodissociation coefficients (J values) and bioactive radiation (UV index, DNA damage, vitamin D production, etc.) can be calculated by TUV model. Radiation propagation through different atmospheric layers (concentric spherical shells for direct sunlight, parallel surface for scattered radiation) is calculated using a rapid two-stream approximation or a multi-stream discrete order scheme. The TUV model requires ozone, albedo, and AOD data to predict UVI.

2.2. data

The forecast values of the total ozone column, surface albedo and AOD is required for prediction of the UVI with TUV Radiation model. Total ozone column and surface albedo data are extracted from the Global Forecasting System (GFS) model with horizontal resolution of 0.5 degree. The GFS is a weather forecast model developed by the National Centers for Environmental Prediction (NCEP).

For AOD forecast values, the WACCM data are used with horizontal resolution of 0.9 degrees latitude and 1.25 degrees longitude. The WACCM model is a comprehensive numerical model that covers the

[2] Goddard Chemistry Aerosol Radiation and Transport
[3] Regional Atmospheric Chemistry Mechanism
[4] Global Forecasting System
[5] Weather Research and Forecasting

altitude range from the ground up to about 500 to 700 km [26, 27, 28, 29]. The outputs of this model are applied to generate regional predictions by the atmospheric chemistry community. The WACCM development is an inter-sectional collaboration that integrates specific aspects of High-Altitude Observatory (HAO), Atmospheric Chemistry Observations and Modeling (ACOM), and the CGD troposphere model using the CESM6 model as a common numerical framework. The CESM2/WACCM model is now running in real-time based on NASA/GMAO GEOS-5 weather forecasts. The WACCM is a large set of CAM47models and includes all the physical parameterizations of the CAM4 model and a finite volume dynamical core [30] for advection tracking.

Due to the lack of access to the actual values of UVI, the OMI data with resolution of 1 degree are assumed as observational data in this study. The UVI data from OMUVBd product of Ozone Monitoring Instrument (OMI) are applied to compare with the predicted values. OMI is a spectrometer near to UV/Visible mounted on NASA's Aura satellite. Aura moves 15 minutes behind Aqua, both of which orbit the Earth in a simultaneous solar polar pattern. Aura was launched on 15 July 2004, and OMI has been collecting data since 9 August 2004. The OMUVBd product is a Level 3 product of the OMI.

2.3. Verification scores

Common statistical measures such as Mean Error (ME), Mean Absolute Error (MAE), Root Mean Squared Error (RMSE), and correlation coefficient (R) are used to validate the forecast values with observational data. Their equations are as follows:

$$ME = \frac{1}{N}\sum_{i=1}^{N}(f_i - o_i) \quad (1)$$

$$MAE = \frac{1}{N}\sum_{i=1}^{N}|f_i - o_i| \quad (2)$$

$$RMSE = \sqrt{\frac{1}{N}\sum_{i=1}^{N}(f_i - o_i)^2} \quad (3)$$

$$R = \frac{\sum_{i=1}^{N}(x_i - \bar{x})(y_i - \bar{y})}{\sqrt{\sum_{i=1}^{N}(x_i - \bar{x})^2}\sqrt{\sum_{i=1}^{N}(y_i - \bar{y})^2}} \quad (4)$$

Where f_i and o_i are the forecast and observation values at i^{th} point, respectively; and N is the total number of points. The closer ME, MAE and RMSE is to 0, the more accurate the forecast is. R ranges from -1 to 1. When forecast and observation are well correlated, the value of R is close to 1.

Binary verification scores included Hit Rate (HR), False Alarm Ratio (FAR), Missing Rate (MR), Threat Score (TS) and Equitable Threat Score (ETS) were used to verify UVI forecast against its corresponding observation. In verification scores listed below, a, b, c and d refer to the numbers of correctly forecast points (hits), incorrect forecasts of occurrence, incorrect forecasts of non-occurrence, and correct forecasts of non-occurrence, respectively:

HR = a/(a+c) (5)

FAR = b/(a+b) (6)

MR = c/(a+c) (7)

TS = a/(a+b+c) (8)

ETS = (a-hits_random)/(a+b+c-hits_random) (9)
where **hits_random**=(a+b)(a+c)/(a+b+c+d).

HR is the ratio of correct forecasts of the occurrence of the phenomenon to the number of times the phenomenon has occurred. It varies between 0 for the worst and 1 for the best forecast. FAR is the ratio of the total number of false predictions of non-occurrence of the phenomenon to the total number of predictions. Therefore, the lower the value of FAR, the better the forecast. MR is the number of unforecasted occurrences of the phenomenon to the total number of occurrences. So, the lower the value of this quantity, the better the forecast. The value of the TS varies between 0 for the worst and 1 for the best forecast. ETS is a positively oriented score and its value is one for a perfect forecast.

For verification the UVI forecasts, the UVI thresholds should be considered. The UVI scale used worldwide conforms to international guidelines for reporting UVI recommended by the World Health Organization. According to risk of harm from unprotected sun exposure, UVI is divided to 5 categories. The UVI from 1 to 2 is low, 3-5 is moderate, 6-7 is high, 8-10 is very high and more than 11 is extreme. UVI is unitless, and the higher the index value is, the greater is the potential for damage to the skin and eye, and the less time it takes to harm. In this study, by considering different thresholds for UVI values, two situations of occurrence and non-occurrence can be considered.

3. Results and Discussion

The UV index depends on latitude and longitude, surface altitude, Solar Zenith Angle (SZA), total ozone column, surface albedo, AOD, and cloudiness in the atmosphere. In this study, dates and stations with clear sky conditions were selected. From the years 2019, 2020 and 2021, several clear sky conditions have been selected at some coastal and island stations of the Persian Gulf and Oman Sea. Thus, 102 case studies have been selected and for each case, the values of total ozone column, surface albedo, and AOD were extracted from the models described in Section 2 and interpolated to the desired points by the bilinear method. The number of 16 synoptic stations located on the coasts and islands of the Persian Gulf and Oman Sea has been selected and the UVI prediction in those stations has been studied.

Due to the lack of access to the actual values of UVI, the OMI data were assumed as observational data and used to compare with the forecast values. Because the UV index variable in the OMUVBd product of OMI is available at the local noontime of each location, the forecast is estimated at 09:00 UTC.

The boxplot to compare the UVI forecast with the corresponding OMI values as observational data in 102 selected case studies is shown in Figure 1. As seen, the UVI forecast data agree with the OMI values and do not differ significantly with each other. The median of forecasted UVI is lower than the median of OMI, and therefore the UVI forecast is underestimated.

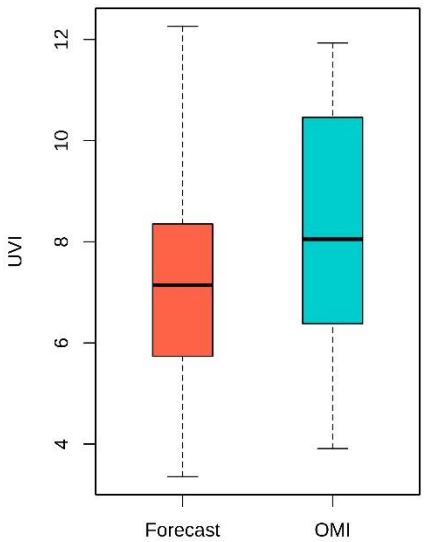

Figure 1. Boxplot of UVI forecast and OMI data

The UVI forecasts and OMI data in each month are averaged and shown in Figure 2. Also, the average of AOD on each month is written above each bar. As seen, the difference between forecast and OMI data is high when the AOD value is high (April and June months). In most months, the predicted UVI value is lower than the OMI value in average. In general, the UVI forecast values and the OMI data are coincident with each other.

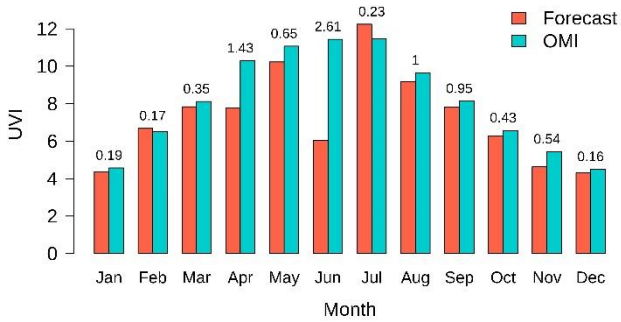

Figure 2. The average values of UVI forecast and OMI data in each month. The numbers above bars are the average of AOD values.

For more detailed verification of the forecast accuracy in different seasons, the ME, MAE, RMSE, and the average value of UVI and AOD in each season are shown in Table 1. As seen, in the warm seasons of the year, when the UVI values are higher than the cold seasons, the forecast error is also high. In addition, the forecast errors have a relation to the AOD values. In this way, in spring and summer, when the AOD value is higher than autumn and winter, the prediction error is also high.

Table 1. Seasonly UVI forecast error.

Season	ME	MAE	RMSE	UVI	AOD
Spring	-2.25	2.44	3.17	10.70	1.26
Summer	-0.01	1.15	1.54	10.82	0.70
Autumn	-0.46	0.51	0.67	6.24	0.52
Winter	-0.12	0.38	0.47	6.71	0.25

The distribution maps of UVI forecast errors in the selected stations are depicted in Figure 3. At each station point, the statistics of ME, RMSE, R and the average value of the AOD are calculated and shown in Figure 3. To calculate the error, the difference between the predicted UVI value using the TUV model and the UVI value from the OMI data as observational data has been calculated. Figure 3d shows the average of AOD data. As shown, the points with higher AOD values (figure(3d) have a higher error and lower correlation coefficient.

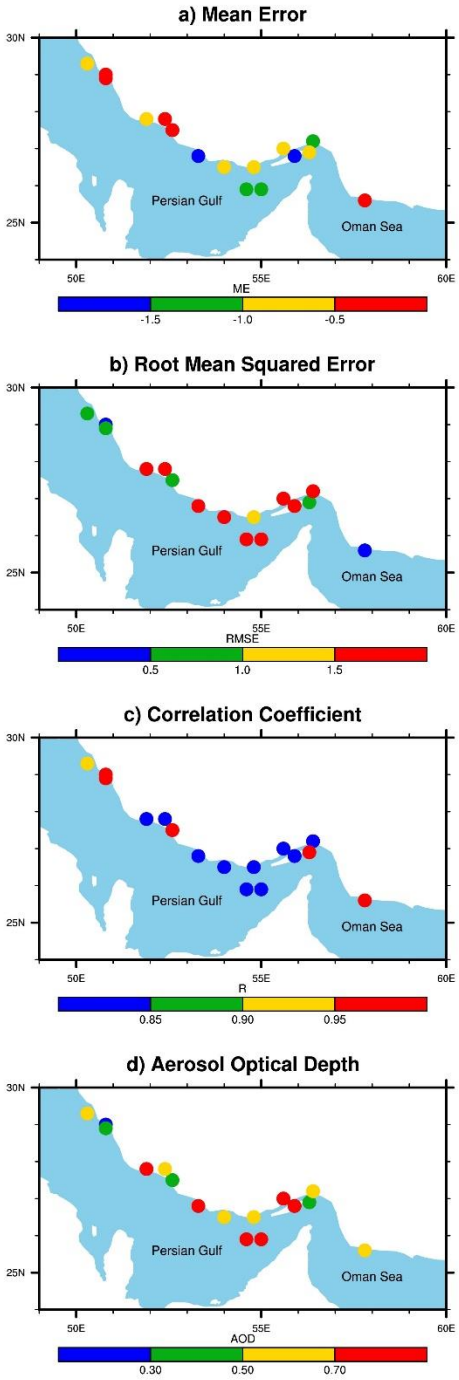

Figure 3. Distribution maps of UVI forecast errors; a) Mean error, b) Root mean squared error, c) Correlation coefficient, d) AOD.

Binary verification scores included HR, FAR, MR, TS and ETS were used to verify UVI forecast against its corresponding observation. Considering that there was no UVI value in the threshold of 1-2 in 102 selected cases, Figure 5 shows the values of the validation scores in the other 4 thresholds. According to Figure 5, the HR, TS and ETS for threshold 3-5 are highest. Also, the upper thresholds show the minimum values of HR, TS and ETS. The FAR and MR for threshold 3-5 are lowest, and the upper thresholds show the maximum values of FAR and MR. Therefore, the better forecast of UVI was at the threshold of 3-5, and the UVI forecast at high thresholds shows more error. Considering that the highest UVI values occur in the warm seasons and the lowest UVI values occur in the cold seasons, it can be concluded that the UVI forecast error is higher in the warm seasons, which is consistent with the results of [31], because in warm seasons, the models can't capture the ozone column and aerosol effects (i.e. dust and smoke) [31].

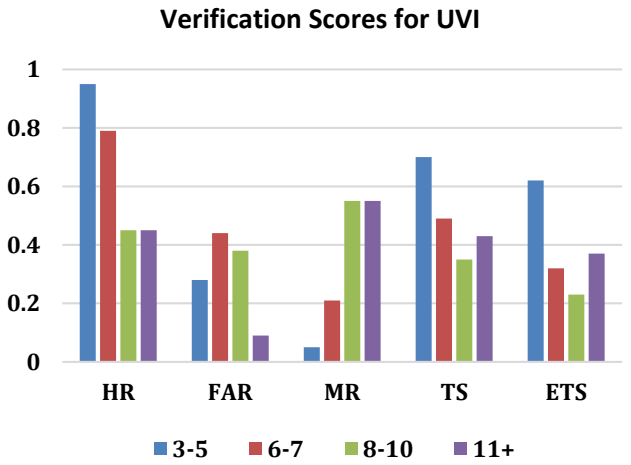

Figure 4. Scores of HR, FAR, MR, TS and ETS of the forecast of UVI for 3-5, 6-7, 8-10 and more than 11 thresholds for 102 case studies.

4. Conclusions

In this study, the Tropospheric Ultraviolet and Visible (TUV) Radiation model was used to forecast the UV index for 102 case studies over coastal stations and islands of the Persian Gulf and Oman Sea in the years 2019, 2020, and 2021. This model requires total ozone column, surface albedo, and aerosol optical depth data to forecast UVI. The total ozone column and albedo forecast values were extracted from the GFS model and AOD forecast values were extracted from the WACCM model and interpolated at desired points. Then, the interpolated data with latitude, longitude, and altitude of the points were given to the TUV model as inputs and UVI forecasts were estimated at different points. Due to the lack of access to the actual values of UVI, the OMI data were used as observational data. Results showed that UVI is higher in the warm seasons than the cold seasons, while UVI forecast error is higher in the warm seasons. Also, when the AOD value is high, the forecast error is high as well, but in general, the UVI forecast is very accurate. In all selected case studies, values of ME, MAE, RMSE, and R are -0.81, 1.07, 1.83, and 0.75, respectively, which indicates the high accuracy of the UVI forecasts.

5. References

[1] Diffey, B.L., 1991, "*Solar ultraviolet radiation effects on biological systems*". Physics in Medicine

& Biology, 36, pp. 299–328. https://doi.org/10.1088/0031-9155/36/3/001.

[2] Lucas, R., McMichael, T., Smith, W., and Armstrong, B., (2006), *"Solar ultraviolet radiation: global burden of disease from solar ultraviolet radiation. In: Prüss-Üstün, A., Zeeb, H., Mathers, C. and Repacholi, M. (Eds.),* World Health Organization Public Health and the Environment Geneva 2006. Environmental Burden of Disease Series 13. Geneva, Switzerland: World Health Organization, p. 250 https://www.who.int/uv/health/solaruvradfull_180706.pdf.

[3] Young, A.R., (2006). *"Acute effects of UVR on human eyes and skin".* Progress in Biophysics and Molecular Biology, 92, pp. 80–85. https://doi.org/10.1016/j.pbiomolbio.2006.02.005.

[4] Webb, A.R., Slaper, H., Koepke, P. and Schmalwieser, A.W., 2011. *"Known your standard: clarifying the CIE erythema action Spectrum".* Photochemistry and Photobiology, 87(2), pp. 483–486. https://doi.org/10.1111/j.1751-1097.2010.00871.x.

[5] McKinlay, A.F. and Diffey, B.L., 1987. *"A reference action spectrum for ultraviolet induced erythema in human skin".* CIE Journal, 6, pp. 17–22.

[6] Herman, J., Huang, L., McPeters, R., Ziemke, J., Cede, A. and Blank, K., 2018. *"Synoptics ozone, cloud reflectivity, and erythemal irradiance from sunrise to sunset for the whole earth as viewed by the DSCOVR spacecraft from the earth–sun Lagrange 1 orbit".* Atmospheric Measurement Techniques, 11, pp. 177–194. https://doi.org/10.5194/amt-11-177-2018.

[7] Erickson D. J., Sulzberger, B., Zepp, R.G. and Austin, A.T., 2015. *"Effects of stratospheric ozone depletion, solar UV radiation, and climate change on biogeochemical cycling: interactions and feedbacks".* Photochem. Photobiol. Sci, 14, pp. 127–148.

[8] Hader, D. P., Kumar, H. D., Smith, R. C. and Worrest, R. C., 2007. *"Effects of solar UV radiation on aquatic ecosystems and interactions with climate change".* Photochem. Photobiol. Sci, 6, pp. 267–285, 10.1039/B700020K.

[9] Smith, R. C., and Cullen, J. J., 1995. *"Effects of UV radiation on phytoplankton".* Reviews of Geophysics, 33, pp. 1211–1223, 10.1029/95RG00801, 10.1029/95RG00801.

[10] Zepp, R., Erickson, D., Paul, Nigel. and Sulzberger, B., 2007. *"Interactive effects of solar UV radiation and climate change on biogeochemical cycling".* Photochemical & photobiological sciences: Official journal of the European Photochemistry Association and the European Society for Photobiology, 6, pp. 286-300. 10.1039/b700021a.

[11] Butchart, N., 2014. *"The Brewer-Dobson circulation".* Reviews of Geophysics, 52, pp. 157–184.

[12] Hegglin, M. I. and Shepherd, T. G., 2009. *"Large climate-induced changes in ultraviolet index and stratosphere-to-troposphere ozone flux".* Nature Geoscience, 2, pp. 687–691, 10.1038/ngeo604.

[13] Bais, A., Tourpali, K., Kazantzidis, A., Akiyoshi, H., Bekki, S., Braesicke, P., Chipperfield, M. P., Dameris, M., Eyring, V., Garny, H., and et al., 2011. *"Projections of UV radiation changes in the 21st century: impact of ozone recovery and cloud effects".* Atmospheric Chemistry and Physics, 11, pp. 7533–7545.

[14] Correa, M. d. P., Godin-Beekmann, S., Haeffelin, M., Bekki, S., Saiag, P., Badosa, J., Jegou, F., Pazmino, A. and Mahe, E., 2013. *"Projected changes in clear-sky erythemal and vitamin D effective UV doses for Europe over the period 2006 to 2100".* Photochem. Photobiol. Sci, 12, pp. 1053–1064.

[15] Bais, A., McKenzie, R., Bernhard, G., Aucamp, P., Ilyas, M., Madronich, S., and Tourpali, K., 2015. *"Ozone depletion and climate change: impacts on UV radiation".* Photochemical & Photobiological Sciences, 14, pp. 19–52.

[16] Brewer, A. W., 1949. *"Evidence for a world circulation provided by the measurements of helium and water vapor distribution in the stratosphere".* Quarterly Journal of the Royal Meteorological Society, 75, pp. 351–363.

[17] Dobson, G., 1956. *"Origin and distribution of the polyatomic molecules in the atmosphere".* Proceedings of the Royal Society of London A: Mathematical, Physical and Engineering Sciences, 236, pp. 187–193.

[18] Holton, J. R., Haynes, P. H., McIntyre, M. E., Douglass, A. R., Rood, R. B. and Pfister, L., 1995. *"Stratosphere-troposphere exchange".* Reviews of Geophysics, 33, pp. 403–439, 10.1029/95RG02097, 10.1029/95RG02097.

[19] Shepherd, T. G., 2008. *"Dynamics, stratospheric ozone, and climate change".* Atmosphere-Ocean, 46, pp. 117–138, 10.3137/ao.460106.

[20] Lamy, K., Josse, B., Portafaix, T., Bencherif, H., Godin-Beekmann, S., et al., 2017. *"Ultraviolet Radiation evolution during the 21st century".* CCMI 2017, Chemistry-Climate Model Initiative Science Workshop, Jun 2017, Toulouse, France. ffhal-01648231f

[21] Madronich, S. and Flocke, S., 1997. *"Theoretical estimation of biologically effective UV radiation at the earth's surface. In: Zerefos, C. S. and Bais, A.F. (Eds.) Solar Ultraviolet Radiation: Modelling, Measurements, and Effects".* Berlin: Springer, pp. 23–48.

[22] Podrascanin, Z., Atlagic, M., Mijatovic, Z. and Sremac, A.F., 2018. *"Uv Index Forecasting in Vojvodina Region".* RAD Conf. Proc. 3, pp. 187–190.

[23] Roshan, D.R., Koc, M., Abdallah, A., Martin-Pomares, L., Isaifan, R. and Fountoukis, C., 2020. *"UV Index Forecasting under the Influence of Desert Dust: Evaluation against Surface and Satellite-Retrieved Data".* Atmosphere, 11, 96. https://doi.org/10.3390/atmos11010096

[24] Lamy, K., Portafaix, T., Josse, B., Brogniez, C., Godin-Beekmann, S., et al., 2019. *"Ultraviolet Radiation modelling using output from the Chemistry Climate Model Initiative".* Atmospheric Chemistry and Physics Discussions, European Geosciences Union, 19(15), pp. 10087–10110.

[25] Krzyścin, J.W., Guzikowski, J., Pietruczuk, A. and Sobolewski, P., 2020. *"Improvement of the 24 hr forecast of surface UV radiation using an ensemble approach".* Meteorol Appl. 27: e1865. https://doi.org/10.1002/met.1865.

[26] Kinnison, D. E., Brasseur, G. P., Walters, S., Garcia, R. R., Sassi, F., Boville, B. A., Marsh, D., Harvey, L., Randall, C., Randel, W., Lamarque, J.-F., Emmons, L. K., Hess, P., Orlando, J., Tyndall, J., and Pan, L., 2007. *"Sensitivity of chemical tracers to meteorological parameters in the MOZART-3 chemical transport model".* J. Geophys. Res., 112, D20302, doi:10.1029/2006JD007879, 2007.

[27] Garcia, R. R., Marsh, D., Kinnison, D. E., Boville, B. and Sassi, F., 2007. *"Simulations of secular trends in the middle atmosphere, 1950-2003".* J. Geophys. Res., 112, D09301, doi:10.1029/2006JD007485.

[28] Marsh, D. R., Mills, M. J., Kinnison, D. E., Lamarque, J. F., Calvo, N., and Polvani, L. M., 2013. *"Climate change from 1850 to 2005 simulated in CESM1 (WACCM)".* Journal of Climate, 26 (19), doi:10.1175/JCLI-D-12-00558.1.

[29] Garcia, R. R., Smith, A. K., Kinnison, D. E., de la Camara, A. and Murphy, D., 2017. *"Modification of the gravity wave parameterization in the Whole Atmosphere Community Climate Model: Motivation and results".* J. Atmos. Sci., 74, 275-291, doi:10.1175/JAS-D-16-0104.1.

[30] Lin, S. J., 2004. *"A "vertically-Lagrangian" finite-volume dynamical core for global atmospheric models".* Mon. Wea. Rev., 132, pp. 2293-2307.

[31] Prasad, S. S., Deo, R. C., Downs, N,. Igoe, D., Parisi A. V. and Soar, J., 2020. "*Cloud Affected Solar UV Prediction with Three-Phase Wavelet Hybrid Convolutional Long Short-Term Memory Network Multi-Step Forecast System*" in IEEE Access, vol. 10, pp. 24704-24720, doi: 10.1109/ACCESS.2022.3153475.